structural health monitoring of composites for aircraft structures

[a]QuEST Global Engineering, Ground Floor, Building-5 B, SEZ (Pritech II), Bangalore, Karnataka - 560 103, India

[b]Department of Aeronautical Engineering, New Horizon College of Engineering, Bangalore, Karnataka - 560 103, India

[c]School of Mechanical and Manufacturing Engineering, University of New South Wales, Sydney, NSW – 2053, Australia

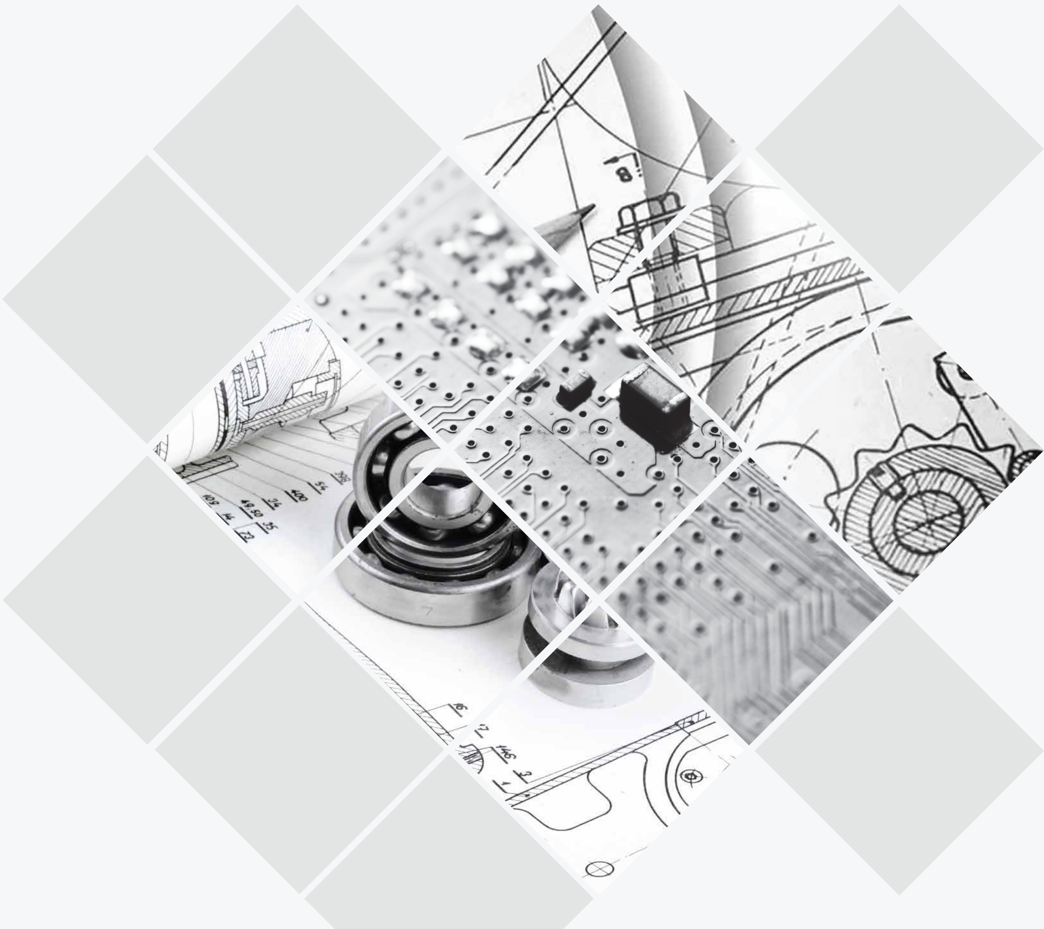

Dr. Raju[a,b,c*]
QuEST Global

contents

Abstract

Failures in smart composite structures are catastrophic due to absence of plastic behaviour. Failures such as delamination and fibre breakages are critical failure modes in composites, which results in significantly reduced strength and structural integrity. An effective structural health monitoring (SHM) system successfully senses the abnormalities bound to occur in the structure with abnormal loading and aggressive environmental conditions.

This paper discusses about Acoustic emission technique where in the minute cracking noise sensed using both piezo-electric and fibre optic sensors. Fibre optic sensors could effectively be used as a sensor to measure Temperature, Strain, Pressure, etc. Surface bonded Piezo-electric and fibre optic sensors – Fibre Bragg Grating (FBG) are used to sense acoustic-emissions (AE), to gain insight into failure initiation and progression. Failure mode discrimination is performed by analysing the AE (signal) waveform and examining various parameters such as peak amplitude, rise-time, signal duration, threshold crossings and elastic energy from individual AE signals. The feasibility of the system is demonstrated in typical in-situ structural health monitoring applications, using AE techniques.

Discussion on an experimental investigation using appropriate ASTM standards would be discussed. This cost-effective approach would minimise excessive weight by having numerous sensors built in one single optical fibre with single input and single output. This effectively could be used in various industries including Aerospace, Marine, Automotive, etc. Using the proposed techniques, different failure modes of composites such as matrix failure, delamination, crack propagation and fibre breakage could be successfully characterized. Due to their low equipment weight and large coverage area, optical fibre AE sensing mechanisms are more suitable for the Aerospace domain.

Keywords: fibre optic sensors; structural health monitoring; delamination; composite failure modes; acoustic mission; piezoelectric sensors

Introduction

Usage of composite materials in Aero/Mechanical/Marine structures presents a challenge in the continuous assessment of the strength and integrity of the structure. The various loads acting on a structure a complex state of stresses in the structure. The process of implementing a damage identification strategy for aerospace, civil and mechanical engineering infrastructure is referred to as structural health monitoring (SHM).This process involves the observation of a structure or mechanical system over time using periodically spaced measurements, the extraction of damage-sensitive features from these measurements and the statistical analysis of these features to determine the current state of system health [1,2]. Acoustic-emission and optical-fibre sensing are passive forms of in-situ structural health monitoring, as no additional excitation is applied to the structure other than the operational load [15].

Fibre optic sensor – Internal refraction technique

Optical fibres can transmit light over a long distance with minimal loss and the properties of the light inside the fibre are not affected by physical parameters outside the fibre. This implies that the fibre can be used as both the sensing element and the communication path for the signal between the sensor and the optical interrogator. The key attributes of Optical fibre sensors (OFS) are immunity to electro-magnetic interference (EMI), intrinsic or extrinsic placement, water and corrosion resistance, low maintenance, ruggedness, smaller size, low cost and they can be multiplexed in parallel or in series. Modern OFS are suitable for the measurement of temperature, pressure, strain, angular rotation speed, acceleration, curvature, flow, refractive index, and many other parameters [3]. Optical fibres consist of a high refractive index core, where broadband light travels as shown in Figure 1. The total internal reflection guides the light is guided inside the core.

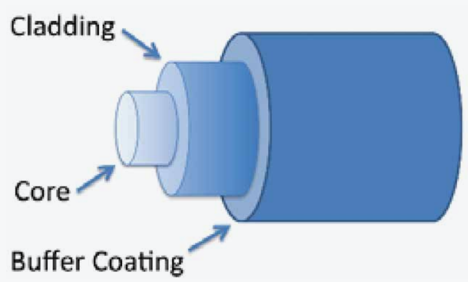

Figure 1: Typical Optical Fibre Cross-section

Acoustic Emission Technique

Acoustic Emission (AE) is compatible with structural composites to be used as trusted Structural Health Monitoring (SHM) technique. When the elastic energy exceeds the critical limit in a loaded structure, a crack occurs and this elastic energy is released rapidly, which is termed as AE. AE measurement is based on the detection of microscopic surface movements from stress waves in a material during the fracture process [4,5]. Traditionally, Piezoelectric AE sensors are mounted on the surface of the structure using an appropriate clamping mechanism. Modern optical fibre AE sensors are capable of sensing AE and could be used as an alternative to piezoelectric sensors. This could result in significant amount of weight savings which is a critical parameter for aircraft structures. However, a the technique needs to be validated against conventional piezo-electric sensors. Based on the extensive literature survey [6-11], the failure values for various AE parameters are given in Table 1.

Failure Mode	Amplitude (dB)	Energy (eu)	Duration (ms)	Rise time (μs)	Frequency (kHz)
Matrix Cracking	40-55	<5000	8-10	N/A	50-150
Interface Debonding	55-65	5000-8000	10-15	1-5	150-350
Fibre breakage	65-85	9000-12000	>15	5-20	350-400
Delamination	90-100	>12000	>25	>20	>450
Fibre pull-out	65-85	N/A	N/A	N/A	0-250

Table 1: AE Failure values for advanced composites

Materials and Methods

Top hat stiffened panels are used out-of-plane load transfer joints, which have high bending stiffness and torsional resistance. This could be generally seen on the Aircraft floor beams. A typical top hat stiffener is shown in Fig 4.

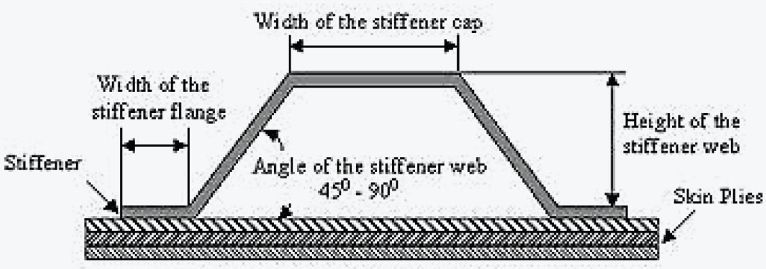

Figure 2: Typical top hat stiffener

For the current study, the specimens are manufactured using Vacuum Assisted Resin Transfer Moulding (VARTM) which is a closed-mould process, providing high strength, high stiffness and good surface finish.

The different fabrics used in this study are E-glass Chopped Strand Mat (CSM) – 451 gsm, Double Bias (DB) – 611 gsm, Vinylester SPV 6036 (FGI) resin and Norex CHM-50 hardener. The layup sequence of the specimens is presented in Table 2. A snapshot of the Top-hat-stiffener specimens manufactured by VARTM is shown in Figure 3. The specimens are cured under the vacuum bag for 24 hours at a temperature of 20°C.

Mould Surface	DB-450	CSM-450	DB-450	CSM-450	DB-450	CSM-450	DB-450	DB-450	Total Thickness
Thickness (mm)	0.26	0.6	0.26	0.6	0.26	0.6	0.26	0.26	**3.1**

Table 2: Laminate Configuration

Figure 3: Top-hat-stiffener manufacturing with VARTM

Experimental Program

The bottom flange of the top hat stiffener was secured using clamps and the displacement load was applied at a rate of 2 mm/min (Cross-head movement).

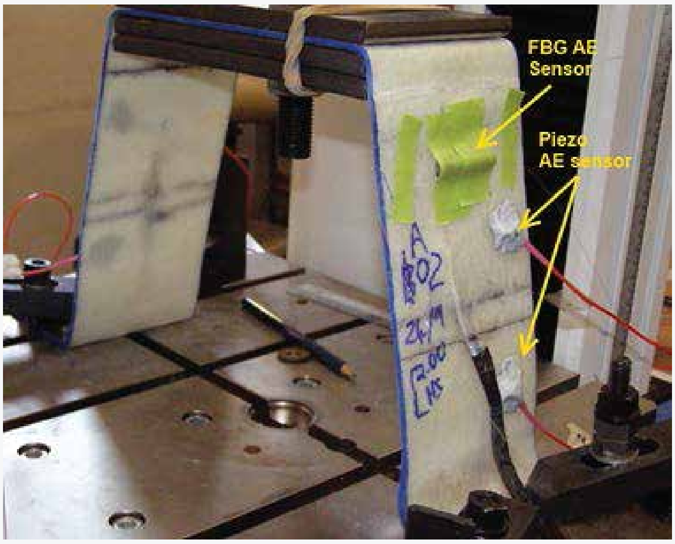

Figure 4: Specimen with attached sensors

AE Set-up- Piezo-electric Sensors

Four-channel AE equipment - DISP, from Physical Acoustic Corp. (PAC) - was used to acquire the stress waves generated by the loaded specimen. For each of the AE signal, parameters such as signal rise time, amplitude, duration of the signal, counts, hits, signal strength and energy released are analysed.

AE Set-up- Fibre optic sensors

In this experimental program, an optical fibre with a single FBG sensor was surface bonded to specimens and the AE was recorded during the testing. A personal computer is connected to a fibre-optic interrogator. Labview 8.0 software was used for recording and analysing the data. It consists of tunable laser system as the interrogation source and a phase shifted fibre Bragg Grating (PS-FBG) as the sensor head. The number of data recorded per second was limited to four, due to the processing power required to handle the large amount of data. The acoustic waveform was automatically saved by a trigger level when its amplitude exceeded a certain level.

Results and Discussion

Load-deflection test results

The Layup consisted of five DB-450 gsm and three CSM-450 gsm layers. The load-deflection behaviour of this layup is shown in Figure 5. An initial stiffness of 1 kN/mm is seen until the first failure (Table 3).

Specimen	First failure Load (kN)	First failure Deflection (mm)	Final failure Load (kN)	First failure Deflection (mm)	Initial Stiffness kN/mm
D01	9.05	11.42	22.01	25.48	0.792
D02	12.48	11.85	29.57	27.04	1.053
D03	9.54	10.37	22.76	23.20	0.920
D05	10.71	10.99	30.83	24.60	0.975

Table 3: Specimen initial and final failure load, deflection and stiffness

Initial failure of the four specimens tested occurred around 11 mm deflection. For specimen 'THS VIP D02', twelve distinguishable load drops are seen on the load-deflection plot in Figure 5. Matrix cracking occurred at 12.48 kN and 11.85 mm deflection.

A significant load drop of 2.76 kN occurred at 13.87 mm deflection. This was a crack between the second and third layers at the radius of the left crown bend. With further application of load, the structure continued to take up the load until the right crown bend failed due to delamination and eccentric loading began on one side of the specimen at 15.66 mm (14.48 kN load). Upon further loading, both the crown bends started to disappear and, at 20 mm (18.91 kN load), the right flange bend suffered a major crack between the fourth and fifth layers. A secondary stiffness started to appear and, at 23.33 mm deflection (24.22 kN load), the left flange bend lost its stiffness and delamination occurred between the fourth and fifth layers. Further loading caused delamination propagation between other layers and the structure finally collapsed at 27.04 mm d and 29.57 kN The laminate sheared away at the left flange base below the edge of the steel plate. Load drops are shown in Figure 5 and the damage process is shown in Figure 6.

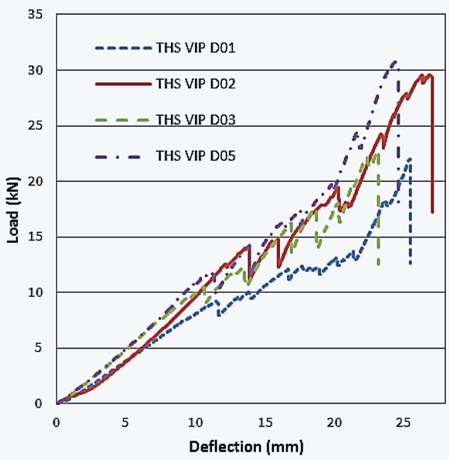

Figure 5: Load deflection plot

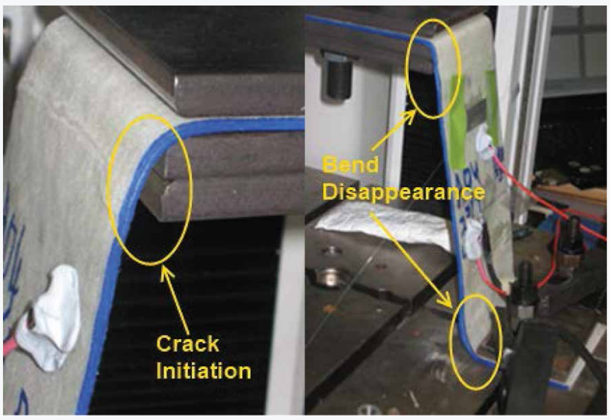

Figure 6: Specimen damage process

Piezo-electric and FBG AE results

Parametric analysis of the piezoelectric and FBG sensor data are discussed in this section. Table 4 presents the amplitude distribution range for the Top hat stiffener specimens. Only a couple of signals reached amplitude of 100 dB. Most were situated between 40–60 dB, indicating crack propagation in the laminate. Four signals which were delamination failures were observed and the rest of the signals were crack-propagation signals. As the peak amplitude for most of the failures is 99 dB, the amplitude parameter is not considered for failure-mode discrimination. Table 5 presents the failure characterisation of the piezoelectric sensor.

Channel	Total	(40-45)	(45-50)	(50-55)	(55-60)	(60-65)	(65-70)	(70-75)	(75-80)	(80-85)	(85-90)	(90-95)	(95-100)
1	4086	652	1625	838	477	272	144	48	17	3	6	0	4
2	7375	1040	3225	1484	762	455	245	107	34	9	5	1	8
3	7165	873	2944	1578	829	439	240	137	70	34	11	0	8
4	9151	1148	3864	2110	1025	529	265	127	54	18	5	1	5

Table 4: Four-channel amplitude distribution ranges (dB)

Failure No.	Time (Sec)	Load (N)	Load drop (N)	Amplitude (dB)	Energy (eu) (1eu=10^{-18}J)	Duration (ms)	Rise Time (ms)	Counts (Threshold Crossings)	Signal Strength	Failure Mode
1	224.66	7571	7	99	5914	25.80	1.61	406	36945024	Matrix Cracking
2	299.83	10818	484	99	6549	18.88	2.74	315	40910904	Delamination
3	320.23	11404	223	99	3927	18.33	8.45	927	24532492	Crack progression
4	345.35	11254	437	99	3654	22.12	0.56	467	22830236	Delamination
5	383.36	12337	72	99	4890	39.38	26.37	2290	41089040	Crack progression
6	422.50	14200	1575	99	10358	68.51	1.43	3039	64706032	Delamination
7	486.50	16150	93	66	54	1.55	0.22	85	536223	Crack progression
8	530.77	17456	631	99	7641	17.23	9.93	410	47732564	Crack progression
9	592.52	19690	257	78	258	6.08	0.22	129	1617729	Crack progression
10	655.54	24699	1122	99	5804	17.70	0.86	347	36260192	Delamination
11	743.00	30345	12457	99	8659	21.64	15.60	1433	54093544	Fibre failure

Table 5: Piezo-sensor Acoustic-emission failure characterisation

The initial failure was thought to be matrix cracking with a small drop in load of 7 N at 224.66 sec, and a high energy release and duration of 5914 eu and 25.80 ms. The major crack occurred at 299.83 sec, delamination failure with a significant drop of 484 N. The signal lasted 18.88 ms and energy released was 6549 eu. The signal at 320.33 sec corresponded to crack propagation with a 437 N drop in the load, but the rise time and counts were just 0.56 ms and 467. A large energy release, of 10358 eu, was observed at 422.50 sec with a load drop of 1575 N corresponding to a delamination failure. The duration and counts were 68.51 ms and 3039, respectively. Further loading caused the cracks to propagate in the laminate. Three peak values were determined at 486.50, 530.77 and 592.52 sec. The signal duration was small compared to the delamination signal. Another major crack occurred at 655.54 sec with a 1122 N drop in load. The parametric values of energy, duration, rise time and counts were 5804 eu, 17.70 ms, 0.86 ms and 347 respectively. Final collapse, an observed drop in load of 12457 N was assumed a fibre failure.

The failure values of the FBG–AE sensor are presented in Table 6. The values are comparatively lower than those for a piezoelectric sensor but the trend is similar to piezo-sensors; failure modes were successfully identified using these values. Only one FBG AE sensor was used, whereas, four piezo-sensors were used. Parameters such as amplitude, energy, duration, rise time and counts are compared with the piezo-sensor values in Figures 7-12. The reasons for low values of FBG AE sensor in comparison with the Piezo sensors could be attributed towards surrounding noise and usage of only one FBG sensors in comparison with four Piezo-electric sensors.

Failure No.	Time (Sec)	Load (N)	Load drop (N)	Amplitude (dB)	Energy (eu) (1eu=10-18J)	Duration (ms)	Rise Time (ms)	Counts (Threshold Crossings)	Failure Mode
1	224.66	7571	7	74.27	13074	15.39	6.87	3231	Matrix Cracking
2	299.83	10818	484	73.45	1048	11.19	3.80	1063	Delamination
3	320.23	11404	223	63.92	386	8.68	0.52	936	Crack progression
4	345.35	11254	437	66.52	1337	3.24	3.66	458	Delamination
5	383.36	12337	72	61.35	276	18.36	1.50	1974	Crack progression
6	422.50	14200	1575	52.10	1308	5.97	2.83	230	Delamination
7	486.50	16150	93	62.08	760	9.78	4.51	840	Crack progression
8	530.77	17456	631	49.31	2453	10.32	1.56	804	Crack progression
9	592.52	19690	257	64.02	1612	9.59	1.90	1112	Crack progression
10	655.54	24699	1122	71.22	227	6.26	2.58	521	Delamination
11	743.00	30345	12457	72.94	1707	10.77	7.33	412	Fibre failure

Table 6:FBG (Fibre optic) Sensor Acoustic-emission failure characterisation

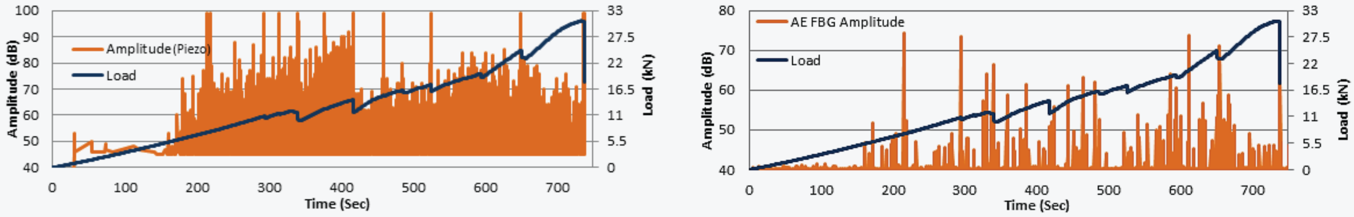

Figure 7: AE comparison of piezo and FBG sensor amplitude

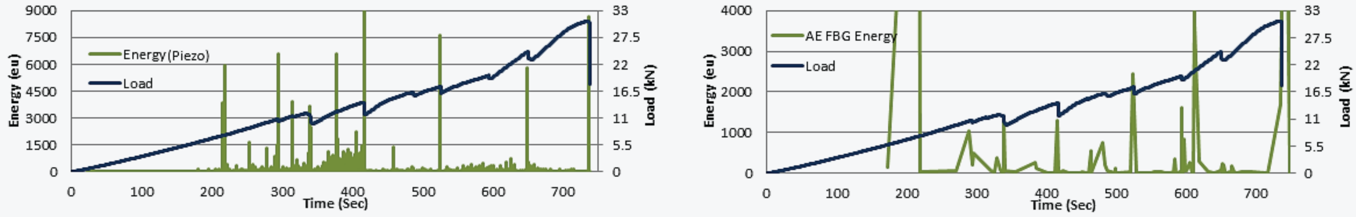

Figure 8: AE comparison of piezo and FBG sensor energy released

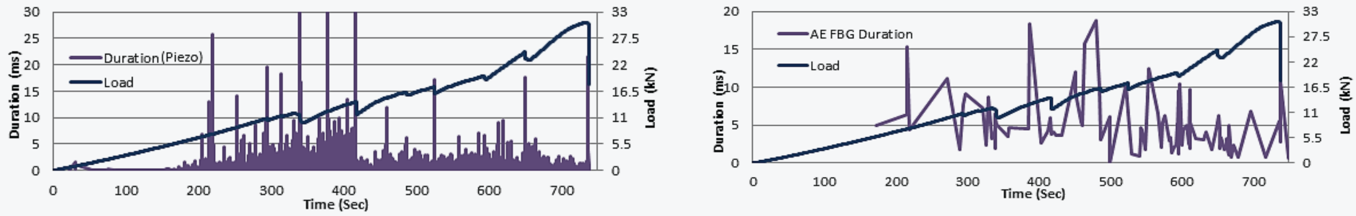

Figure 9: AE comparison of piezo and FBG sensor signal duration

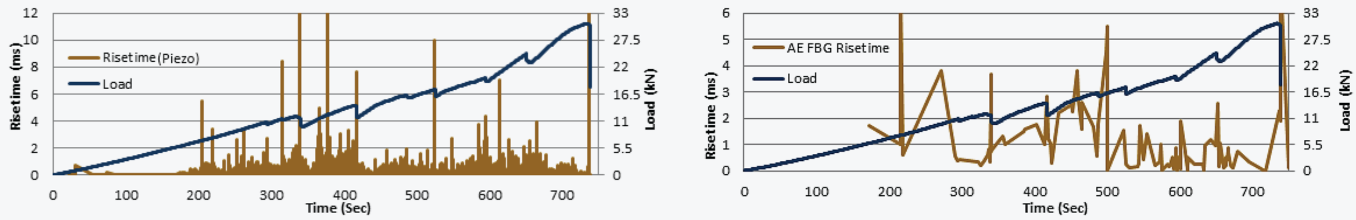

Figure 10: AE piezo and FBG sensor signal rise time comparison

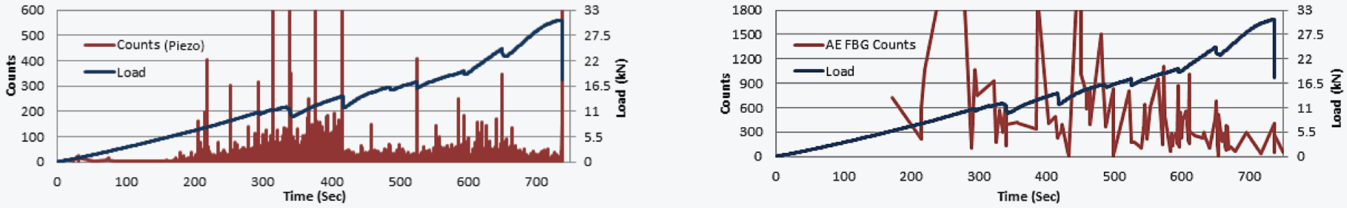

Figure 11: AE piezo and FBG sensor count comparison

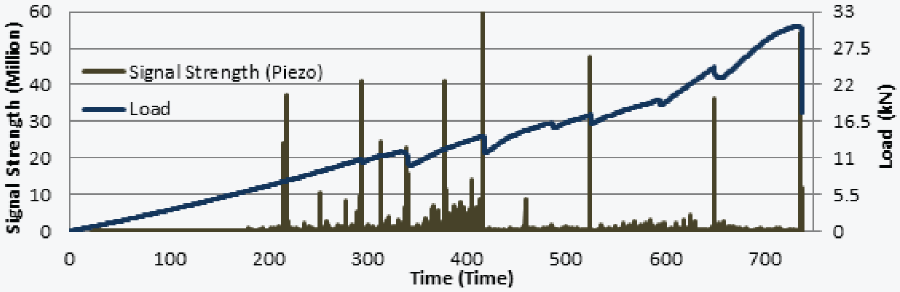

Figure 12: AE piezo-sensor signal strength

The overall damage process could be characterised into three distinctive zones. Figure 13 shows the cumulative counts vs. time and load vs. time plots.

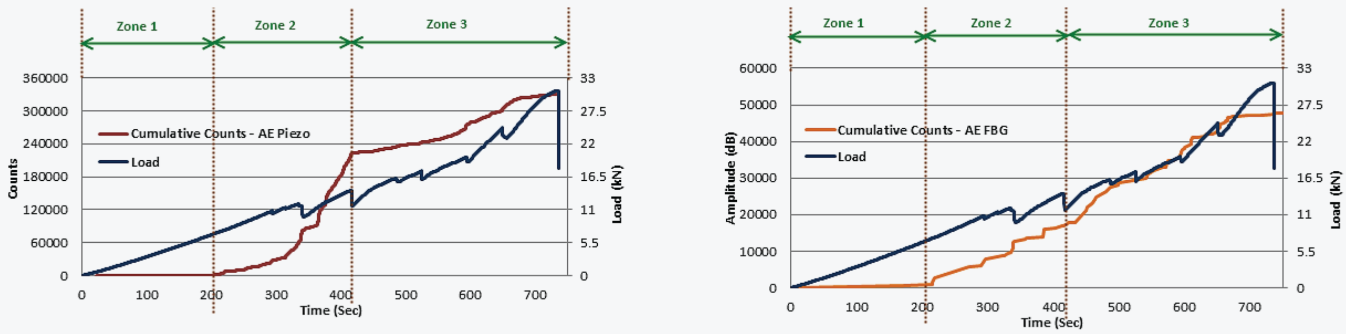

Figure 13: AE piezo and FBG sensor cumulative counts and load v. time plots

Zone 1 covers up to 210 sec, where limited AE activity is observed, because of environmental noise and machine vibration. The number of counts recorded in this zone was 2395. Zone 2 corresponds to the time between 210 and 413 sec, where a steep slope that indicates extensive damage in the structure is observed. There were 211,051 counts within a span of 203 sec and most critical failures, which proved to be delaminations, occurred during this stage. Zone 3 consisted mainly of crack propagation and an ultimate failure between 413 and 743 sec. The slope of the curve was lower with 115,905 counts within a span of 330 sec. The histogram of hits v. time and the plot of cumulative hits v. time for the piezo-sensor are shown in Figure 14. Comparing the three stages, it is evident that stage two had higher rate of hits, indicating large damage to the structure.

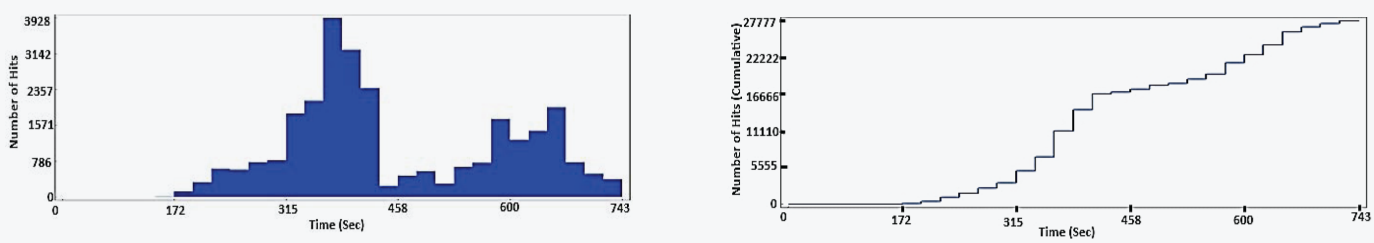

Figure 14: Piezo-sensor cumulative hits and load v. time plot

Conclusion

Experimental Failure characterization of advanced composite structures has been carried out by using surface bonded Piezo electric and fibre optic (FBG) Acoustic Emission sensors. Multiple failure modes were successfully characterized. Two different types of AE sensing mechanisms, conventional piezoelectric sensors and fibre-optic AE sensors were used to obtain AE signals during the damage process. The different analyses of standard piezo-sensor AE signal parameters, FBG-AE signal parameters all yielded indications of changes correlating with the growth of damage in the composite laminate. The results of FBG-AE sensors were compared with the piezo-electric sensors and the failure analysis was satisfactory.

The conclusions could be summarised as:

- Fibre optic sensors have immense potential which yet need to be used in the industry for various applications. In the current study, conventional Piezo-sensors and modern FBG-AE sensors were used to assess and analyse the different failure modes in composite structures
- The individual failure modes such as Matrix Cracking, Debonding, Delamination and Fibre fracture were successfully discriminated using the Parametric analysis of AE signals
- Only one Fibre optic sensor was used. Additional fibre optic AE sensors might be required for efficient validation of Piezo-electric AE sensors with statistical validation
- Based on the comparisons between piezo-electric AE sensor and fibre optic FBG AE sensor, it can be deduced that the FBG sensor could effectively replace the piezo-sensor, thus minimising the bulky equipments. This is more suitable for aerospace applications

Acknowledgement

The author would like to thank Prof. Gangadhara Prusty (UNSW, Sydney, Australia), Dr. Asrul Azmi (Universiti Teknologi Malaysia) and Prof. G.D. Peng (UNSW, Sydney, Australia) for their continuous support during the course of this research. The authors would also like to thank Mr. David Lyons (Seaflyer Pty. Ltd., Gold Coast, Australia) and EMP Composites (Sydney, Australia) for both, manufacturing the specimens and providing valuable suggestions & technical support.

References

1) C.R. Ferrar and K. Worden, An introduction to Structural Health Monitoring, Philosophical Transactions of the Royal Society A, 365, 2007, 303-315.

2) H.C.H. Li, I. Herszberg , A.P. Mouritz, C.E. Davis and S.C. Galea, Sensitivity of embedded fibre optic Bragg grating sensors to disbonds in bonded composite ship joints, Composite Structures, 66, 2004, 239-248.

3) W. Staszewski, C. Boller and G. Tomlinson, Health monitoring of aerospace structures: Smart sensor technologies and signal processing, John Wiley & Sons, Ltd, England, 2004, ISBN 0-470-84340-3.

4) B. Muravin. Acoustic emission science and technology, Journal of Building and Infrastructure Engineering of the Israeli Association of Engineers and Architects, 2009.

5) R.G. Liptai and D.O. Harris, Acoustic emission-an introductory Review, Materials Research and Standards, 11(3), 1971, 8-10.

6) C. Ageorges , K. Friedrich , T. Schuller and B. Lauke, Single-fibre Broutman test: fibre – matrix interface transverse debonding, Composites: Part A, 30, 1999, 1423–1434.

7) S. Barre and M.L. Benzeggagh, On the use of acoustic emission to investigate damage mechanisms in glass fibre-reinforced polypro pylene, Composites Science and Technology, 52, 1994, 369–376.

8) S. Benmedakhene, M. Kenane and L. Benzeggagh, Initiation and growth of delamination in glass/epoxy composites subjected to static and dynamic loading by AE monitoring, Composites Science and Technology, 59, 1999, 201–208.

9) C.A. Barnes and G. Ramirez, Acoustic emission testing of carbon fiber composite offshore drilling risers, The Sixth International Symposium on Acoustic Emission from Composite Materials. San Antonio: American Society for Non-destructive Testing Inc, 1998,13–22.

10) J.M. Berthelot and J. Rhazi, Acoustic emission in carbon fibre composites, Composites Science and Technology, 37, 1990, 411–428.

11) L. Li and J.H. Zhao, The monitoring damage growth processes in glass fiber reinforced composite by amplitude analysis, Second International Symposium on Acoustic Emission from Reinforced Composites Montreal: Reinforced Plastics/Composites Institute, 1986, 90–95.

13) R.A. Shenoi and G.L. Hawkins, An investigation into the performance characteristics of top-hat stiffener to shell plating joints, Composite Structures, 30, 1995, 109–121.

14) A.R. Dodkins, R.A. Shenoi and G.L. Hawkins, Design of joints and attachments in FRP ship structures, Marine Structures, 7, 1994, 364–398.

15) Raju, B.G. Prusty, D.W. Kelly, D. Lyons, G.D. Peng, Top hat stiffeners: a study on keel failures. Ocean Engineering, 37, 2010, 1180–1192.

16) Raju, B.G. Prusty, D.W. Kelly, D. Lyons, G.D. Peng, Failure characterisation of L-bend curved composite laminates, Transactions of Royal Institute of Naval Architects (RINA) Part B2, International Journal of Small Craft Technology, 152, 2010, 93-105.

About QuEST Global

QuEST Global is a focused global engineering solutions provider with a proven track record of over 17 years serving the product development & production engineering needs of high technology companies. A pioneer in global engineering services, QuEST is a trusted, strategic and long term partner for many Fortune 500 companies in the Aero Engines, Aerospace & Defence, Transportation, Oil & Gas, Power, Healthcare and other high tech industries. The company offers mechanical, electrical, electronics, embedded, engineering software, engineering analytics, manufacturing engineering and supply chain transformative solutions across the complete engineering lifecycle.

QuEST partners with customers to continuously create value through customer-centric culture, continuous improvement mind-set, as well as domain specific engineering capability. Through its local-global model, QuEST provides maximum value engineering interactions locally, along with high quality deliveries at optimal cost from global locations. The company comprises of more than 7,000 passionate engineers of nine different nationalities intent on making a positive impact to the business of world class customers, transforming the way they do engineering.

QUEST

BORN TO ENGINEER

http://quest-global.com